

2

TECHNICAL REPORT NO. 8

AD-A275 505



TO

The Office of Naval Research
Contract No. N00014-91-J-1414

DTIC
ELECTE
FEB 08 1994
S E D

**A MODELING STUDY OF THE EFFECT OF
STRESS STATE ON VOID LINKING DURING
DUCTILE FRACTURE**

A. B. Geltmacher°, D. A. Koss°, P. Matic* and M. G. Stout+

°Dept. of Metals Science and Eng., The Pennsylvania State University,
University Park, PA 16802

*Mech. of Materials, Code 6382, Naval Research Laboratory,
Washington, DC 20375

+MTL-5, Los Alamos National Laboratory, Los Alamos, NM 87545

For
ORA&I <input checked="" type="checkbox"/>
AB <input type="checkbox"/>
enced <input type="checkbox"/>
ion

By	
Distribution /	
Availability Codes	
Dist	Avail and / or Special
A-1	

DTIC QUALITY INSPECTED 8

**Reproduction in Whole or in Part is Permitted
For Any Purpose of the United States Government
Distribution of this Document is Unlimited**

94 2 07 07 5

3488 94-04231

**Best
Available
Copy**

REPORT DOCUMENTATION PAGE			Form Approved OMB No. 0704-0188	
<small>Public reporting burden for this collection of information is estimated to average 1 hour per response, including the time for reviewing instructions, searching existing data sources, gathering and maintaining the data needed, and completing and reviewing the collection of information. Send comments regarding this burden estimate or any other aspect of this collection of information, including suggestions for reducing this burden, to Washington Headquarters Services, Directorate for Information Operations and Reports, 1215 Jefferson Davis Highway, Suite 1204, Arlington, VA 22202-4302, and to the Office of Management and Budget, Paperwork Reduction Project (0704-0188), Washington, DC 20503</small>				
1. AGENCY USE ONLY (Leave blank)		2. REPORT DATE January 28, 1994		3. REPORT TYPE AND DATES COVERED Technical Report
4. TITLE AND SUBTITLE A Modeling Study of the Effect of Stress State on Void Linking During Ductile Fracture			5. FUNDING NUMBERS	
6. AUTHOR(S) A. B. Geltmacher, D. A. Koss, P. Matic, and M. G. Stout				
7. PERFORMING ORGANIZATION NAME(S) AND ADDRESS(ES) Department of Materials Science and Engineering The Pennsylvania State University University Park, PA 16802			8. PERFORMING ORGANIZATION REPORT NUMBER Report No. 8	
9. SPONSORING/MONITORING AGENCY NAME(S) AND ADDRESS(ES) Office of Naval Research 800 N. Quincy Street Arlington, VA			10. SPONSORING/MONITORING AGENCY REPORT NUMBER	
11. SUPPLEMENTARY NOTES				
12a. DISTRIBUTION/AVAILABILITY STATEMENT Distribution of this document is unlimited.			12b. DISTRIBUTION CODE	
13. ABSTRACT (Maximum 200 words) Specimens containing arrays of through-thickness holes are used to model aspects of void linking during ductile, microvoid fracture. Specifically, the contrasting deformation and fracture behavior of sheet specimens containing either pairs or "pseudo"-random arrays of equi-sized holes is examined in both uniaxial and equal-biaxial tension utilizing experiment as well as computer simulation. Our results show for this plane-stress situation that hole linking is always caused by flow localization within the ligaments between neighboring holes. The imposed strains to initiate flow localization and subsequent ligament failure are sensitive to stress state (uniaxial versus biaxial), strain hardening, and the location of the neighboring hole(s). A significant observation is the influence of stress state on the multidirectionality of hole linking paths. As a result, increasing the biaxial component of the stress-state increases the number of holes that can participate in a hole-linking process increases. A related and subtle implication to microvoid fracture is that the strain range over which void linking occurs decreases with increasing triaxiality of the stress state; in effect, after the initiation of void linking, its propagation is accelerated under biaxial or triaxial tension.				
14. SUBJECT TERMS Ductile Fracture, Void Linking, Multiaxial Stress States.			15. NUMBER OF PAGES 33	
			16. PRICE CODE	
17. SECURITY CLASSIFICATION OF REPORT	18. SECURITY CLASSIFICATION OF THIS PAGE	19. SECURITY CLASSIFICATION OF ABSTRACT	20. LIMITATION OF ABSTRACT	

A MODELING STUDY OF THE EFFECT OF STRESS STATE ON VOID LINKING DURING DUCTILE FRACTURE

A. B. Geltmacher^o, D. A. Koss^o, P. Matic^{*} and M. G. Stout⁺

^oDept. of Metals Science and Eng., The Pennsylvania State University, University Park, PA 16802

^{*}Mech. of Materials, Code 6382, Naval Research Laboratory, Washington, DC 20375

⁺MTL-5, Los Alamos National Laboratory, Los Alamos, NM 87545

ABSTRACT

Specimens containing arrays of through-thickness holes are used to model aspects of void linking during ductile, microvoid fracture. Specifically, the contrasting deformation and fracture behavior of sheet specimens containing either pairs or "pseudo"-random arrays of equi-sized holes is examined in both uniaxial and equal-biaxial tension utilizing experiment as well as computer simulation. Our results show for this plane-stress situation that hole linking is always caused by flow localization within the ligaments between neighboring holes. The imposed strains to initiate flow localization and subsequent ligament failure are sensitive to stress state (uniaxial versus biaxial), strain hardening, and the location of the neighboring hole(s). A significant observation is the influence of stress state on the multidirectionality of hole linking paths. As a result, increasing the biaxial component of the stress-state increases the number of holes that can participate in a hole-linking process increases. A related and subtle implication to microvoid fracture is that the strain range over which void linking occurs decreases with increasing triaxiality of the stress state; in effect, after the initiation of void linking, its propagation is accelerated under biaxial or triaxial tension.

INTRODUCTION

Increasing the triaxiality of the applied stress state normally decreases the fracture strain of structural alloys, as is readily evident from several proposed failure criteria; see ref's. 1-3, for example. For alloys failing due to damage accumulation in the form of microvoids, this dependence implies a sensitivity to void nucleation, void growth, and/or void linking on the imposed stress state. The strain to nucleate voids is known to decrease as the triaxiality of the stress state increases.^{1, 4-10} Both experiments and analyses also indicate that the growth rate of voids increases rapidly at high degrees of stress triaxiality.¹¹⁻¹⁶ In contrast, the influence of stress state on void linking is not well established.

An accelerated rate of void linking under biaxial or triaxial stress-states is suggested by observations of multiaxial fracture due to microvoiding in titanium and zirconium alloy sheet containing hydrides.^{17,18} In both of these studies, specimen fracture occurred within a small strain increment after void nucleation during equal biaxial tensile deformation; in contrast, specimen failure was much more "gradual" in uniaxial tension, i.e., a large strain increment accumulates after void nucleation but before eventual fracture (which also occurred at a higher void volume fraction).^{17,18} These results suggest that the critical void volume fraction necessary to trigger massive void linking and specimen failure is sensitive to stress state; specifically, the susceptibility to void linking appears to increase within biaxial or triaxial stress-states.

In the present study we examine the effect of stress state on void linking. Modeling three-dimensional void/pore-linking process with two-dimensional arrays of through-thickness holes, we have performed both experiments and computer simulation to examine the deformation and fracture behavior of specimens which contain either pairs of holes or arrays of 63 holes. The specimens were deformed and modeled in either uniaxial or equal-biaxial tension. Of special interest is the combined

effect of stress state and spatial distributions of holes (i.e. hole "microstructures") on deformation within the interhole ligaments, hole linking, and specimen fracture.

The relationship of the mechanisms of three-dimensional void-linking to the two-dimensional hole-linking behavior in this study deserves comment. We recognize that the linking of voids can occur either by stable void growth to coalescence or by the localization of deformation within the intervoid ligament such that it causes ligament failure. This latter form of void linking is akin to the "void-sheet" mechanism of ductile fracture.¹⁹⁻²¹ As has been demonstrated in previous studies examining the deformation and fracture behavior of sheet specimens containing holes,²²⁻²⁴ our experiments strongly bias hole linking to occur by a flow localization phenomena. Likewise, our computer simulation assumes plane-stress conditions to model the experimental results, and thus it also biases hole linking to occur by flow localization of the ligament between the holes. As will be discussed later, it is important to recognize that hole linking under plane-strain conditions also occurs by deformation localization between holes.^{22,23} This study, as well as most other studies using two-dimensional hole linking to model three-dimensional void linking, is thus a limiting case.

EXPERIMENTAL AND COMPUTATIONAL APPROACH

A) Experimental Procedure

The material selected in the present study is 1 mm thick sheet of 3003 aluminum (1.2Mn-0.12Cu-remainder Al), which has been annealed (after hole drilling) at 350°C for 2 hours followed by an air cool. Deformation of the sheet occurs in the plane-stress condition and is characterized by a strain-hardening exponent $n = d\ln(\sigma - \sigma_0)/d\ln\epsilon \cong 0.20$. The material has a grain size of $\cong 110 \mu\text{m}$; this corresponds to at least 14 grains across the smallest interhole ligament.

In the first part of the study, sheet specimens containing pairs of 1.6 mm diameter holes were tested in both uniaxial and equal-biaxial tension. Specimens

with hole spacings of 1, 2 and 3 hole diameters were examined. In uniaxial tension, the holes oriented at either 0° or 90° to the rolling direction. Equal-biaxial tension tests were performed by using a hemi-spherical punch (50.8 mm diameter) and die. The surface between the specimen and punch was lubricated with PTFE sheets and molybdenum-disulfide grease to insure equal-biaxial conditions in the region of the sheet containing the holes. In all cases, the initial equivalent strain rate was 10^{-3} s^{-1} . In all experiments, the specimens were gridded utilizing a photoresist technique in order that the localization strains between the holes could be measured and to confirm the applied strain path.

In the second part of the study, experimental tests were performed on sheet specimens containing arrays of through-thickness 1.6 mm diameter holes machined into a 102 mm diameter circular area centrally located in the specimen. The distance from the edge of the specimen to the nearest hole was at least 50 mm. The test conditions were selected so that the area fraction of holes was 0.02 in all cases. The arrays may be categorized as either regular or "pseudo"-random. The regular arrays are based on hexagonal and triangular unit cells with interhole spacings of 8.7 mm and 11.2 mm, respectively, as shown in Figure 1. The second type of hole array is termed "pseudo"-random in that the holes are constrained by a minimum allowable interface spacing. This spacing defines the distance from a given hole over which no other hole is allowed to be present. As shown in Figure 1, the effect of hole clustering can be examined by generating arrays of 63 holes with two different values (1.6 mm and 3.2 mm) of the minimum allowable interhole spacing. It follows that the degree of hole clustering increases as the minimum allowable interhole spacing decreases. Figure 1 indicates visually that the degree of clustering decreases as the minimum allowable interhole spacing increases. For the "pseudo"- random conditions, five different arrays were generated at each spacing.

Equal-biaxial tension testing of the specimens containing the hole arrays was performed on a 229 mm hydraulic bulge test machine using specimens 254 mm x 254 mm square with the holes centrally located in a circular region 102 mm in diameter. The equal-biaxial strain path was confirmed by examination of grids on blank specimens subjected to the bulge testing. Tests of the specimens with through-thickness holes were performed using the material arrangement shown in Figure 2. As shown, a sheet of 0.15 mm PTFE was placed below the aluminum specimen in order to prevent the hydraulic pressure from leaking through the specimen. Above the specimen, a sheet of 0.76 mm thick 316 stainless steel was used to confine the hydraulic fluid and to keep the failure of the aluminum from being catastrophic. In between the aluminum and steel, another sheet of 0.15 mm thick PTFE, sprayed with a molybdenum-disulfide lubricant, was placed in order to reduce the amount of friction during the tests. The tests were performed by loading the specimens in small (~ 0.005) equivalent-strain⁺ increments at an average initial, equivalent strain-rate of 10^{-3} s^{-1} . Uniaxial tension was performed on large (254 mm wide) sheets as a basis of comparison to the behavior in equal-biaxial tension. Identical hole arrays were tested for both uniaxial and equal biaxial loading paths.

B) Computer Simulation of Specimens with Pairs of Holes

The effects of hole spacing, sheet work-hardening, and applied deformation path on the strain localization behavior of specimens with pairs of holes was also examined by finite element modeling using the ABAQUS implicit code. The effect of hole spacing was examined by modeling specimens with a pair of equal-sized, circular holes that were spaced either 1, 2 or 3 hole diameters apart. Two-dimensional meshes were generated using PATRAN for the above geometries. The mesh size

⁺ The equivalent strain, $\bar{\epsilon}$, was calculated by assuming a plastically isotropic material in which case $\bar{\epsilon} = \sqrt{2/3} [(\epsilon_1 - \epsilon_2)^2 + (\epsilon_2 - \epsilon_3)^2 + (\epsilon_3 - \epsilon_1)^2]^{1/2}$

ranged from 794 to 1139 elements for the specimen geometries, with a refined mesh surrounding the holes. As mentioned before, the simulations were performed in plane-stress conditions by using the CPS8 elements in ABAQUS. The mesh is deformed in either uniaxial or equal-biaxial tension by the application of the proper displacement boundary conditions.

The effect of sheet work-hardening was examined by varying the stress/strain responses of the material in the finite element code. The stress/strain response for 3003 aluminum was modeled by the equation

$$\sigma = \sigma_0 + K\varepsilon^n \quad (1)$$

where σ_0 is the yield strength, K is a constant and n is the strain-hardening exponent. For the 3003 aluminum used in this study, the yield strength and strain-hardening exponent were 15 MPa and 0.20, respectively. In order to examine the effect of strain-hardening on the deformation and flow localization behavior near the holes, "model" materials were chosen with the same yield strength as the 3003 aluminum but with strain-hardening exponents of 0.05 and 0.50.

RESULTS AND DISCUSSION

In the initial part of this study, we examine the deformation and fracture response within a single ligament separating a pair of through-thickness holes in sheet specimens subjected to far-field stress-states of either uniaxial or equal biaxial tension. In the case of uniaxial tension ligament failure occurs preferentially by flow localization between those holes which are oriented such that the axis between the hole centers is nearly normal to the direction of applied stress. This behavior is consistent with previous plane-stress experimental and computational results.²²⁻²⁴ Thus, the present experiments and computational modeling is confined to pairs of holes with an interhole axis normal to the stress axis. This case represents that condition which promotes hole linking at the smallest imposed far-field strain.

The following sections describe the flow localization process which results in hole linking either in the uniaxial or equal-biaxial tension. As will be described, computational modeling, validated by experiments, is primarily used to explore flow localization behavior between pairs of holes as a function of far-field strain path (uniaxial vs. equal biaxial tension), hole spacing, and matrix strain hardening. The computational predictions contain significant implications pertaining to the behavior of specimens containing arrays of holes, and experimental results describing the deformation and fracture behavior of specimens containing pseudo-random arrays of 63 holes are described in the subsequent section.

A) Experimental and Computational Simulation of Specimens Containing Pairs of Holes

1. Initial Observations

The flow localization behavior within an interhole ligament between a pair of holes was examined using both experiment and computer simulation. Experimental validation was performed using 3003 aluminum specimens that were deformed until a localized neck could be observed visually between the pair of holes; the local strain values (major and minor principal strains in the plane of the sheet) were measured from the grids just prior to and after the onset of flow localization. Such an experimental criterion is identical to that used in identifying localized necking in sheet metal deformation.²⁵ Since subsequent specimen deformation accumulates strain very rapidly within the "localized" ligaments, the onset of observable flow localization within an interhole ligament is usually tantamount to ligament fracture and hole linking.

In the computer model, flow localization within the interhole ligament was determined by comparing, at small steps of applied boundary displacement, the effective strain increment, $d\bar{\epsilon}_{lg}$, at an element centrally located within the ligament to that in an element located >14 hole diameters away from the ligament, $d\bar{\epsilon}_m$.

Furthermore, we define the onset of flow localization in the computer model as that critical far-field strain value, $\bar{\epsilon}_m^*$, at which deformation concentrates within the ligament such that $d\bar{\epsilon}_{lig} / d\bar{\epsilon}_m \geq 10$.

As an initial comparison between experiment and computational prediction, Figure 3 shows the predicted specimen strain-values within the central 12.7 mm of the tensile specimen agree reasonably well with those determined experimentally at the onset of observable flow localization within the interhole ligament. Figure 3 also shows, as will be discussed later, (a) that increasing interhole spacing delays the onset of flow localization and (b) that the experimental and computer results are in good agreement.

Further support for the validity of the computational results is shown in Figure 4 by comparing the local strain distributions between a pair of holes at a specific macroscopic, applied strain. Figure 4 shows that the spatial distributions of these local strain values also show good agreement between the experimental measurements and the computer simulation. Figure 4 also indicates that the local strain state at the onset of flow localization is nearly plane strain, over the central ~70% of the ligament, even though the imposed macroscopic strain path is uniaxial tension. Similar experimental and computational results were observed for specimens containing a pair of holes and deformed in equal-biaxial tension. Therefore, we conclude that a significant effect of the presence of neighboring holes is to force the interhole ligament into a plane-strain deformation path. This occurs for both uniaxial and equal biaxial tension and for hole spacings up to 3 hole diameters.

2. The Effect of Applied Strain Path on Flow Localization

As just noted, the dominant strain path along which an interhole ligament deforms is plane-strain tension even though the applied stress state is either uniaxial or equal-biaxial tension. However, as shown in Figure 5, computer modeling shows that the

critical applied, far-field ("macroscopic") strain $\bar{\epsilon}_m^*$, needed to initiate flow localization between a pair of holes is greater in equal-biaxial tension than for the case of uniaxial tension where the pair of holes is "ideally" oriented normal to the stress axis. For the case of a material with a strain-hardening exponent of 0.20 and hole spacing of 2 hole diameters, Figure 5 indicates that $\bar{\epsilon}_m^* \approx 0.025$ in uniaxial tension but has a much larger value of $\bar{\epsilon}_m^* \approx 0.045$ in equal-biaxial tension. This effect is also readily apparent in the computational data which depict the local strain distributions near the hole. All of the strain components are spatially diffuse around the holes in equal-biaxial tension; in contrast, in uniaxial tension the strains concentrate readily between holes oriented normal to the stress axis.²⁶ The ability of equal-biaxial tension to diffuse deformation is consistent with a larger $\bar{\epsilon}_m^*$ -value needed to initiate flow localization within the interhole ligament. Thus, flow localization within the ligament between neighboring holes is easier to achieve between "properly" oriented holes in uniaxial tension than equal-biaxial tension.

3. Effect of Hole Spacing

The effect of hole spacing on flow localization between holes, shown in Figure 6, indicate that as the interhole spacing increases, the magnitude of $\bar{\epsilon}_m^*$ and thus the strain-value for hole linking, increases for both uniaxial and equal-biaxial tension. Figure 6 shows that in both uniaxial and equal-biaxial tension, $\bar{\epsilon}_m^*$ increases by roughly a factor of three as the interhole spacing increases from 1 to 3 hole diameters.

As noted previously, the uniaxial tensile case modeled is based on a pair of holes oriented for easy hole linking (Figure 4). Obviously, if the interhole axis is inclined to the stress axis, flow localization will be delayed to larger $\bar{\epsilon}_m^*$ -values. Thus, in uniaxial tension there must be a biasing of flow localization and ligament failure in specimens containing arrays of holes. Specifically, during specimen deformation, those holes

oriented such that the interhole axes are nearly normal to the stress axis will link first as the specimen is deformed. This suggests that failure in uniaxial tension should occur on preferred fracture paths which, due to hole-linking considerations, will be nearly normal to the stress axis.

The results in Figures 5 and 6 indicate that the applied macroscopic strain required to cause flow localization within the interhole ligaments increases as stress biaxiality increases and hole spacing increases. However, there remains the question of the combined influence of interhole spacing and stress state. Based on computations for specimens containing pairs of holes, Figure 7 indicates the following two observations: (1) as expected, for a given hole spacing, the $\bar{\epsilon}_m^*$ value (and ligament fracture strain) are greater in equal-biaxial tension than for the uniaxial-tension case, and (2) surprisingly, these far-field strain values are more sensitive to hole spacing in equal-biaxial tension than uniaxial tension. The far-field strains versus hole-spacing lines in Figure 7 are essentially linear but have different slopes. This implies that, at least in specimens containing arrays of holes, hole interaction effects may be more sensitive to interhole spacing in multiaxial tension than in uniaxial tension. This is consistent with computational predictions that void interaction effects between spherical voids spaced one void diameter apart are large only at high degrees of stress triaxiality.¹⁶

4. Effect of Sheet Work-Hardening

Flow localization phenomena are known to be very sensitive to matrix strain-hardening as well as strain-rate hardening. In the present study, 3003 Al exhibits essentially no strain-rate hardening at room temperature. Thus, thus a strain-rate insensitive computer simulation was used to examine the effect of strain hardening on the flow localization behavior within the interhole ligament between a pair of holes. Figure 8 shows that, as is expected from previous experimental studies,²³ increasing

the strain-hardening exponent of the matrix increases the $\dot{\bar{\epsilon}}_m$ -value in uniaxial tension, Figure 8a, as well as in equal-biaxial tension, Figure 8b. These results are consistent with the expectation that increasing strain hardening diffuses the strain concentration around the hole. Computational results showing spatial distributions of strains near holes as a function of matrix strain hardening confirm such an expectation.²⁶

The combined influence of matrix flow behavior and applied strain path on flow localization between pairs of holes is depicted in Figure 9. As expected, $\dot{\bar{\epsilon}}_m$ is very sensitive to strain hardening and increases rapidly with increasing strain hardening. Intuitively, this might be expected. As is well known, increasing the strain hardening exponent makes the material less susceptible to the development of extremely localized deformation. In addition, we observe a second effect in that at large n -values, (e.g., $n=0.5$), the "material" is not nearly as sensitive to stress state effects. In this case, the values of $\dot{\bar{\epsilon}}_m$ are nearly equivalent between uniaxial and equal-biaxial tension. In contrast, the effect of stress state on $\dot{\bar{\epsilon}}_m$ is more pronounced for smaller n -values, (e.g., $n=0.20$). We believe that this indicates the dominant role of strain hardening, as opposed to differences in strain path, in controlling flow localization.

Finally, we wish to comment on the strain values at the onset of flow localization between a pair of holes. For sheet deformation in uniaxial tension a localized necking instability should occur at a maximum principal strain value, ϵ_1 , approximately twice the work-hardening exponent.^{27,28} In plane strain, the necking instability strain should equal the n -value. Figures 3 through 6 indicate flow localization (necking instability) occurs at a local effective strain values of $\simeq 0.1$ to 0.3 . An analysis of these data²⁶ suggest that localized necking occurs within the interhole ligament at either a value of $\epsilon_1 = 2n = 0.4$ at the hole surface, which is in uniaxial tension, or at $\epsilon_1 = n = 0.2$ in the center of the ligament, where the stress state is one of plane strain. This is illustrated in Figure 4. Thus, flow localization appears to obey the classic localized

necking criterion for a range of hole spacings irregardless of the imposed far-field strain path (i.e., uniaxial versus equal-biaxial tension). Greater far-field strains are necessary in equal-biaxial tension, as opposed to uniaxial tension, to produce the same ligament strain because the strain gradients are not as steep. This implies that multiaxial tensile strain paths are not as effective as plane-strain tension or uniaxial tension in inducing the necessary ligament strains to initiate flow localization between holes (or voids).

5. Some Implications

The failure behavior of the ligament between a pair of neighboring holes contains significant implications applicable to hole linking within an array of holes and to void linking within a three-dimensional void population. First, as mentioned in the Introduction, the use of two-dimensional models of voids based on through-thickness holes in sheet specimens strongly biases the hole linking to a process of flow localization within the interhole ligament. It should also be recognized that even materials with high strain hardening are susceptible to deformation localization within interhole ligaments (note $\bar{\epsilon}_m^*$ values for $n=0.50$ in Figure 9). Hole growth to impingement simply does not occur. Thus, from the standpoint of void linking, the present results should relate to local shear instabilities which generate the three-dimensional void-sheet mode of void linking and failure. While interhole ligament flow localization is pronounced in our plane-stress model, experiments examining hole linking in plane strain also indicate a pronounced susceptibility to hole linking by flow localization.²² The tendency for deformation localization between holes can be readily understood in terms of the ease of configuring a planar imperfection band which is inclined so as to initiate a shear localization process.^{29,30}

The second significant implication is the recognition that hole linking between a pair of holes in uniaxial tension is directional; i.e., it is sensitive to the orientation of the

holes to the major principal stress axis. For example, if the hole pair axis is oriented normal to the direction of uniaxial stress, flow localization and ligament failure occur at comparatively small far-field strains in uniaxial tension; see Figures 5,7, and 9.

However, other experiments indicate shear localization between holes in uniaxial tension is very sensitive to deviations from the hole configuration chosen here.^{22,31} Thus, in a specimen containing many randomly oriented hole-pairs there will be hole configurations where plasticity dictates easy flow localization, as when a pair of holes is oriented normal to the stress axis in our plane stress case. Conversely, flow localization will be retarded as neighboring holes misorient from the "easy localization" orientation. Thus hole linking paths within specimens containing arrays of the holes will necessarily be directional in uniaxial tension, occurring near planes $\sim 90^\circ$ to the stress axis in the plane-stress case (or $\sim \pm 45^\circ$ in the plane-strain case). Both of these are observed experimentally.^{22,23}

The third significant implication is the obvious retarding effect of increasing interhole spacing and strain hardening on flow localization. This effect appears somewhat more pronounced in equal biaxial tension than in uniaxial tension (Figures 7 and 9). The implication is that high strength alloys which often have low strain hardening exponents will be very susceptible to hole/void linking by flow localization rather than void growth even in triaxial tension. It is probably no accident that the void-sheet type of void linking has been most commonly reported in relatively high strength steels and aluminum alloys¹⁹⁻²¹ with a comparatively small strain-hardening exponent.¹⁹⁻²¹

Finally and perhaps most important, the above results imply that in a specimen containing an array of hole pairs with a range of misorientations to the stress axis, hole linking in uniaxial tension will proceed over a wide range of strains. Evidence for the behavior, and its implications, are best illustrated in the next section which describes the behavior of specimens containing arrays of 63 holes.

B) Multiple-Hole Experiments

1. On the Multidirectionality of Hole Linking Paths

Experimental observations of specimens containing 2 vol. pct. of 63 holes indicate, as in the two-hole experiments, that strain-induced hole linking is always preceded by the localization of deformation within interhole ligaments. During specimen extension, visual observation indicates that the flow localization process appears to occur rather abruptly between linking holes, or among groups of linking holes. The result is ligament failure and linking occur within a fraction of the holes present before the specimen fails.

As implied from the pair-of-holes specimens, a principal effect of the applied stress-state on hole linking, within an array of holes, is the directional nature of the hole linking paths as linking proceeds. This is readily apparent in a visual examination of deformed specimens in which flow localization initiates in such a manner as to form networks of paths between certain holes. As schematically illustrated in Figure 10, the flow localization and subsequent hole linking paths among the "linking" holes in an equal-biaxial specimen are "multi-directional;" i.e., they have no preferred orientation. This is obviously a result of multi-directional nature of the in-plane stresses and strains during equal-biaxial tension. Under such conditions, interhole flow-localization and subsequent fracture of the ligaments between holes depends almost solely on the spacing between the holes; hole orientation does not appear to be a major factor. As a result, more than 50% of the holes participate in the hole linking process shown in Figure 10.

In contrast, Figure 10 also shows the localization paths and subsequent hole linking between the linking holes in an uniaxial specimen with an identical hole array; in this case hole linking is strongly biased to paths nearly perpendicular ($\pm \sim 15^\circ$) to the loading axis. Thus, in uniaxial tension, hole linking is confined to preferred planes and

depends on both the spacing and the orientation of neighboring holes, as was found previously.^{22,23} As hole linking initiates and small bands of enhanced local deformation are created neighboring regions may be shielded, as has been recently discussed by Becker and Smelser.²⁴ The interactions between neighboring bands will be more competitive in uniaxial tension than in equal biaxial tension. This effect and the natural tendency for flow localization to occur between holes oriented normal to the stress axis results in a pronounced path dependence to hole linking in uniaxial tension. When compared to equal-biaxial tension, far fewer holes (~25%) are able to participate in hole linking at specimen failure in uniaxial tension. This suggests the following implication for the influence of stress state on void linking: increasing stress triaxiality accelerates void linking due to the increasingly multidirectional character of the linking paths. As a result, a larger fraction of void sites participate in the linking process.

An important, but less obvious, implication of the above results is that hole linking will occur over a much larger range of strain values for specimen failure in uniaxial tension than in equal-biaxial tension. Given the multidirectionality of linking paths in equal-biaxial tension, once hole linking initiates, specimen failure will likely occur after a relatively small strain increment, given the high fraction of holes which link and the "efficiency" or cooperative nature of the linking process. In contrast, although hole linking initiates at smaller strains between certain hole pairs in uniaxial tension (Fig. 7), the preferred hole-linking path requirement implies a large increment of additional strain to link holes oriented "on" the linking path but spaced far apart. Thus, the features illustrated in Figures 7 and 10b compete to create a hole linking process which is more gradual in uniaxial tension than in equal-biaxial tension.

Experimental support for the acceleration of void linking in equal-biaxial tension is shown in Figure 11 in which the void nucleation strain, $\bar{\epsilon}_N$, and specimen fracture strain $\bar{\epsilon}_f$, are compared for a titanium with different hydrogen contents.¹⁷ These data

indicate that specimen fracture in equal-biaxial tension occurs soon after $\bar{\epsilon}_N$ is reached (where $\bar{\epsilon}_N$ is defined as that effective strain where a significant void density, 10^2 voids/mm², is detected). In this case $\bar{\epsilon}_N / \bar{\epsilon}_f \approx 0.95$. In contrast, the uniaxial tensile response is such that a large strain increment accumulates after 10^2 /mm² voids are detected; thus in uniaxial tension, $\bar{\epsilon}_N / \bar{\epsilon}_f \approx 0.6$ and void linking is much more gradual. In fact, given the comparatively small differences in void nucleation strains between uniaxial and equal biaxial tension, see Figure 11, it is likely that the major influence of stress state on the hydrogen embrittlement of Ti sheet is a result of accelerated void linking due to the multidirectionality of linking paths (see Figure 6 of ref 17).

2. The Influence of Hole Clustering

Our results, based on the behavior of a pair of holes, indicate that hole linking is very sensitive to hole clustering. Specifically, at a given strain-hardening exponent hole linking is promoted by a decreased interhole spacing. The effect of hole clustering in promoting hole linking under uniaxial tension is well known.²²⁻²⁴ In the present study, using specimens containing arrays of 63 holes, we can increase the degree of hole clustering by decreasing the minimum allowable interhole spacing. Results from such experiments, shown in Figure 12, indicate that hole clustering, which increases as S/D decreases (see Figure 1), also accelerates flow localization within interhole ligaments in both uniaxial and equal-biaxial tension. Hole linking is promoted by hole clustering, regardless of stress state, since ligament fracture results from flow localization.

Figure 12 also illustrates the problem using regular arrays of voids to model microvoid ductile fracture. The large intervold spacing of such an array results in an unrealistically large macroscopic strain to induce void linking, at least by the flow localization process.

Finally we draw attention to the contrast in behavior of specimens containing arrays of 63 holes with those containing pairs of holes. At the same minimum interhole spacing the onset of flow localization occurs at a smaller far-field strain in the 63-hole specimen. Presumably due to long range interaction effects within the array, the hole array acts to promote flow localization. This effect points out an obvious limitation of relating the behavior of a single ligament between a relatively isolated hole pair to that of a population of ligaments within an array of holes.

SUMMARY

In the present study we examine certain features of three-dimensional void linking by two-dimensional modeling using sheet specimens containing arrays of through-thickness holes. We, and others^{1,16,32}, believe that hole interaction effects in two dimensions are more pronounced than void interaction effects in three dimensions. In the current research, hole interaction effects are further enhanced by the use of sheet specimens, which are known to be very susceptible to flow localization and localized necking phenomena.¹⁹⁻²¹ Thus, we wish to emphasize that the current results relate most directly to the form of void linking which occurs due to plastic flow localization within the intervoid ligaments. The "void sheet" process is a good example of such a void linking phenomenon, as are cases where planes of locally high void (or pore) content can trigger void linking due to deformation localization.^{33,34}

With this in mind, we propose that our results suggest that three-dimensional void linking (due to flow localization) is sensitive to stress state as follows:

(1) The initiation of void linking between neighboring voids is retarded by stress triaxiality. The results of the present study suggest that a larger macroscopic level of strain is needed to develop flow localization in the intervoid ligament at a given void

spacing and matrix strain hardening as the degree of triaxiality is increased; see Figure 9.

(2) The propagation of void linking is promoted by high degrees of stress triaxiality, resulting from the increasingly multidirectional nature of the void linking paths; see Figure 3. This assumes a spatially uniform stress and strain field which does not bias the fracture plane. Thus, void linking will be governed primarily by intervoid spacing (and size) at high triaxiality; such void linking is expected to be "efficient", involving a high fraction of available voids. In contrast, the propagation of void linking under uniaxial strain conditions depends on both the directionality of the linking path and the spacing to the nearest favorably oriented void. This results in a directional void linking path in uniaxial tension. As a result, void linking should be gradual with considerable damage accumulation in the form of void growth, local flow instabilities, and ligament fractures before specimen failure. Previous experimental results support such a hypothesis.

(3) Void linking is promoted by void clustering in both uniaxial and equal-biaxial tension, as is shown in Figure 11. The present results do not indicate whether or not void clustering accelerates void linking even more as stress triaxiality increases.

(4) Void linking is inhibited by the material strain-hardening capability, as is depicted in Figure 9. This is due to the ability of a material with a high strain-hardening exponent to diffuse the strain around the holes. As a result, a larger applied macroscopic strain will be needed to cause flow localization and failure of the ligaments between voids.

In summary, our experiments suggest that much of the dependence of "flow-localization-induced" void linking on stress state can be understood in terms of the directionality of void-linking paths. The number of viable linking paths increases with increasing stress biaxiality. The linking path issue influences the "efficiency" of the void linking process and thus the ease with which accumulated damage is self

propagating. It also suggests that, once voids nucleate, the propagation of void linking and fracture can occur within a small strain increment at high levels of stress triaxiality. As such, the material becomes less tolerant to internal damage. Increasing matrix strain hardening and inhibiting void clustering will retard the onset of such a void linking process and effectively enhance fracture resistance.

ACKNOWLEDGMENTS

We wish to acknowledge the support of the Office of Naval Research, the Naval Research Laboratory, and the Office of Basic Energy Sciences, Division of Materials Sciences, U.S. Department of Energy (MGS) for providing financial support for this study.

REFERENCES

1. P. F. Thomason, Ductile Fracture of Metals, Pergamon Press, New York (1990).
2. S. E. Cliff, P. Hartley, C. E. N. Sturges, and G. W. Rowe, Int. J. Mech. Sci. 32, 1 (1990).
3. J. W. Hancock and D. K. Brown, J. Mech. Phys. Solids, 31, 1 (1983).
4. A. S. Argon and J. Im, Metall. Trans. A, 6A 839 (1975).
5. J. W. Hancock and A. C. Mackenzie, J. Mech. Phys. Solids, 24, 147 (1976).
6. S. H. Goods and L. M. Brown, Acta Metall., 27, 1 (1979).
7. F. M. Beremin, Metall. Trans. A, 12A, 723 (1981).
8. G. LeRoy, J. D. Embury, G. Edward, and M. F. Ashby, Acta Metall. 29, 1509 (1981).
9. A. Brownrigg, W. A. Spitzig, O. Richmond, D. Teirlinck, and J. D. Embury, Acta Metall. 31, 1141 (1983).
10. D. Kwon and R. J. Asaro, Metall Trans. A 21A, 117 (1990).
11. A. R. Rice and D. M. Tracey, J. Mech. Phys. Solids 17, 201 (1969).

12. B. Budiansky, J. W. Hutchinson and S. Slutsky in *Mechanics of Solids* (Pergamon Press, Oxford), 1982, p. 13.
13. C. J. Worswick and R. J. Pick, *J. Mech. Solids* 38, 601 (1990).
14. B. Marini, F. Mudry, and A. Pineau, *Eng. Frac. Mech.* 22, 989 (1985).
15. R. Becker, A. Needleman, O. Richmond and V. Tvergaard, *J. Mech. Phys. Solids* 36, 317 (1988).
16. C. L. Hom and R. M. McMeeking, *J. Appl. Mech.* 56, 309 (1989).
17. R. J. Bourcier and D. A. Koss, *Acta Metall.* 38, 2091 (1984).
18. Fan Yunchang and D. A. Koss, *Metall. Trans. A*, 16A, 675 (1985).
19. T. B. Cox and J. R. Low, *Metall. Trans.* 5, 1457 (1974).
20. J. W. Hancock and A. C. Mackenzie, *J. Mech. Phys. Solids* 24, 147 (1976).
21. G. T. Hahn and A. R. Rosenfeld, *Metall. Trans.* 6A, 653 (1975).
22. E. M. Dubensky and D. A. Koss, *Metall. Trans. A*, 18A, 1887 (1987).
23. P. E. Magnusen, E. M. Dubensky, and D. A. Koss, *Acta Metall.* 36, 1503 (1988).
24. R. Becker and R. E. Smelser, *J. Mech. Phys. Solids* (in print).
25. A. K. Ghosh and S. S. Hecker, *Metall. Trans. A* 6A, 1065 (1975).
26. A. Geltmacher, Ph.D. Thesis, The Pennsylvania State University, 1994.
27. R. Hill, *J. Mech. Phys. Solids* 1, 19 (1952).
28. J. W. Hutchinson and K. W. Neale, in *Mechanics of Sheet Metal Forming: Material Behavior and Deformation Analysis* edited by D. P. Koistinen and N-M. Wang, Plenum Press, London, 1978, p. 127.
29. H. Yamamoto, *Int. J. of Fracture* 14, 347 (1978).
30. M. Saje, J. Pan, and A. Needleman, *Int. J. Fract.* 19, 163 (1982).
31. R. J. Bourcier and D. A. Koss, in *Advances in Fracture Research*, Pergamon Press, N.Y., 1981, p. 7.
32. P. F. Thomason, private communication, 1993.
33. R. J. Bourcier, D. A. Koss, R. E. Smelser, and O. Richmond, *Acta Metall.* 34, 2443 (1986).
34. R. Becker, *J. Mech. Phys. Solids*, 35, 577 (1987).

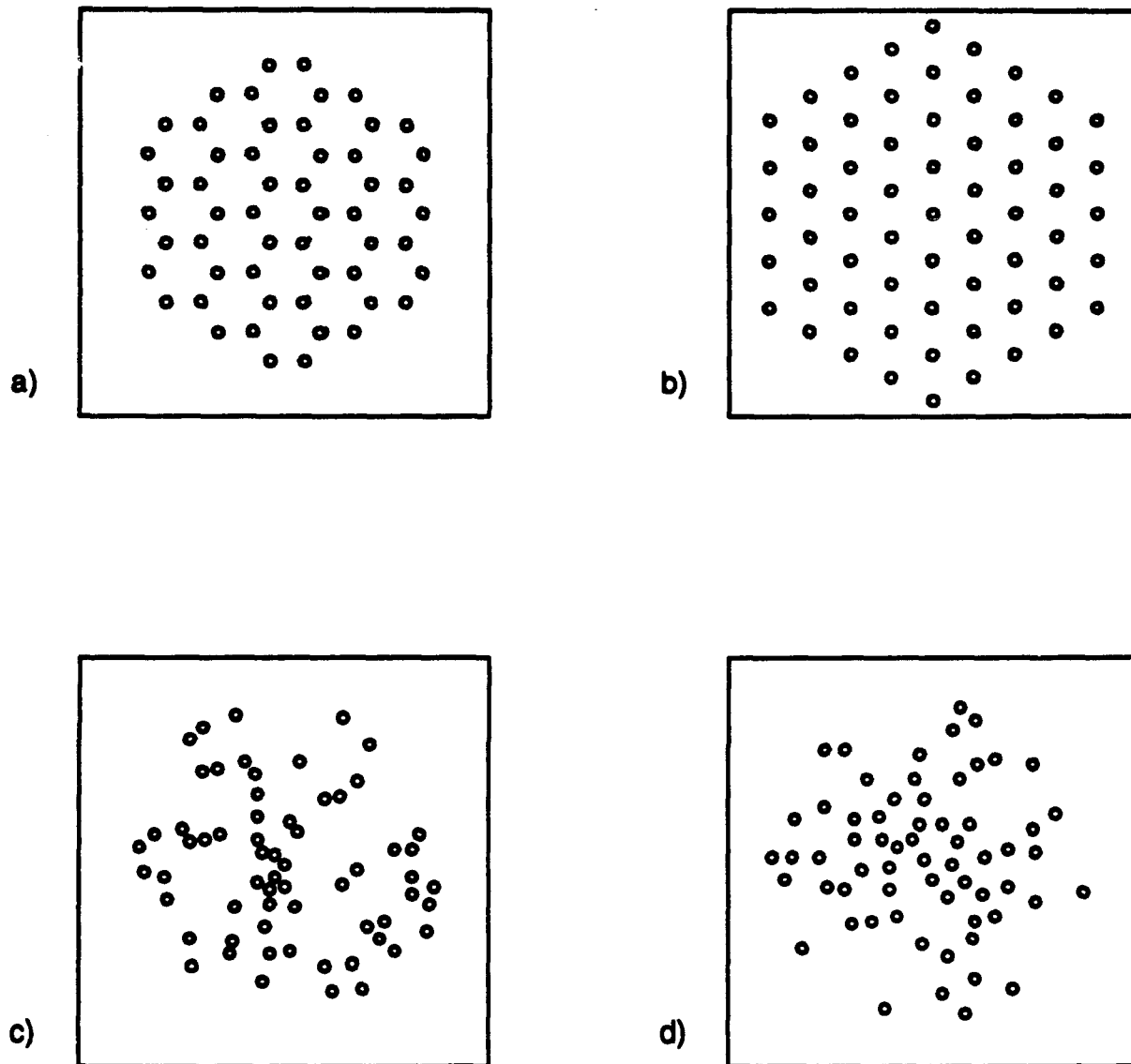


Figure 1: Examples of the specimen hole arrays examined in the present study. The hexagonal and triagonal regular arrays are shown in a) and b), respectively. The "pseudo"-random arrays are for minimum allowable hole spacings normalized by hole diameter of c) $S/D = 1$ and d) $S/D = 2$.

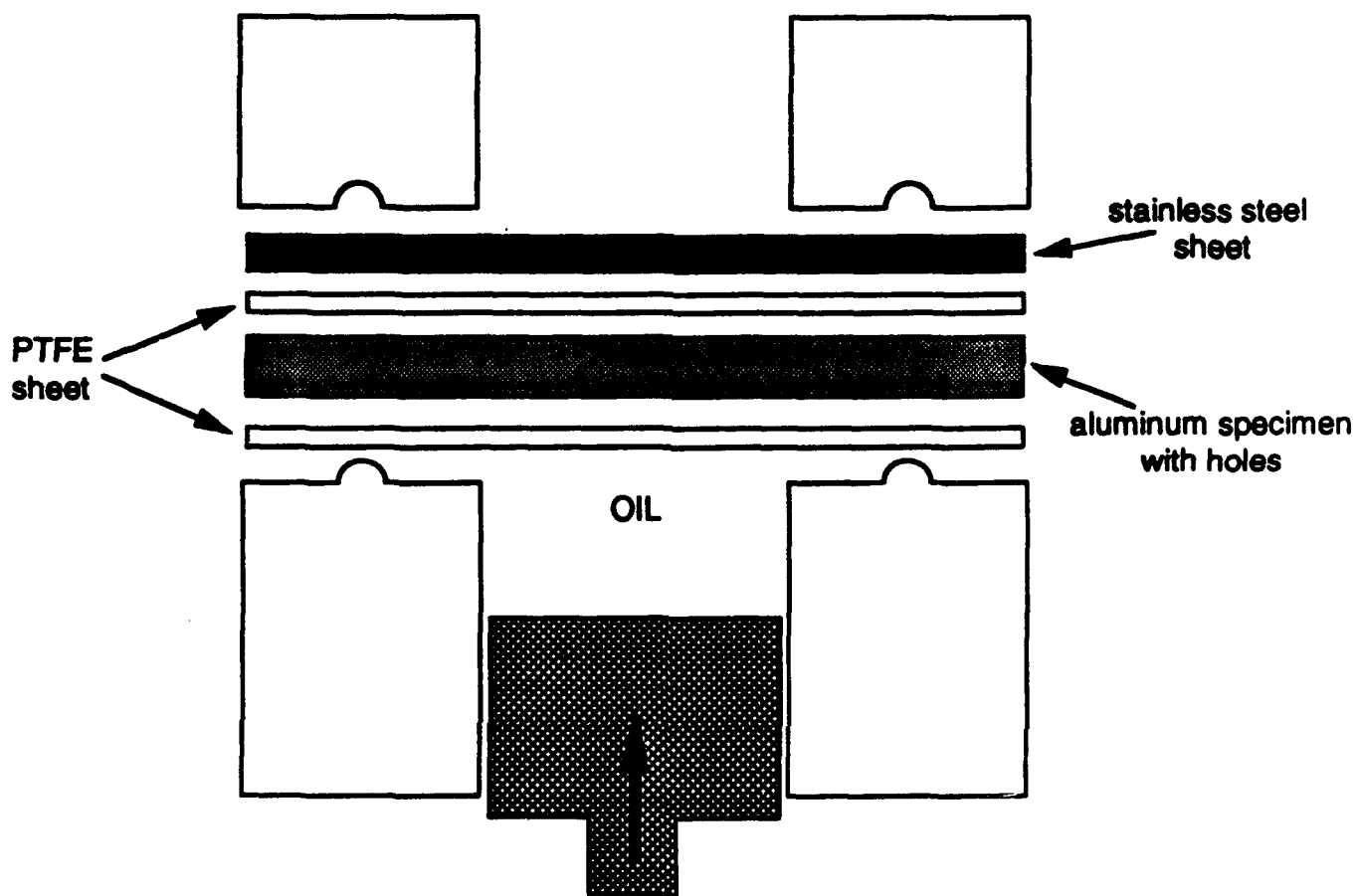


Figure 2. A schematic diagram of the experimental configuration used in the present study to test specimens with through-thickness holes using a hydraulic-bulge test machine.

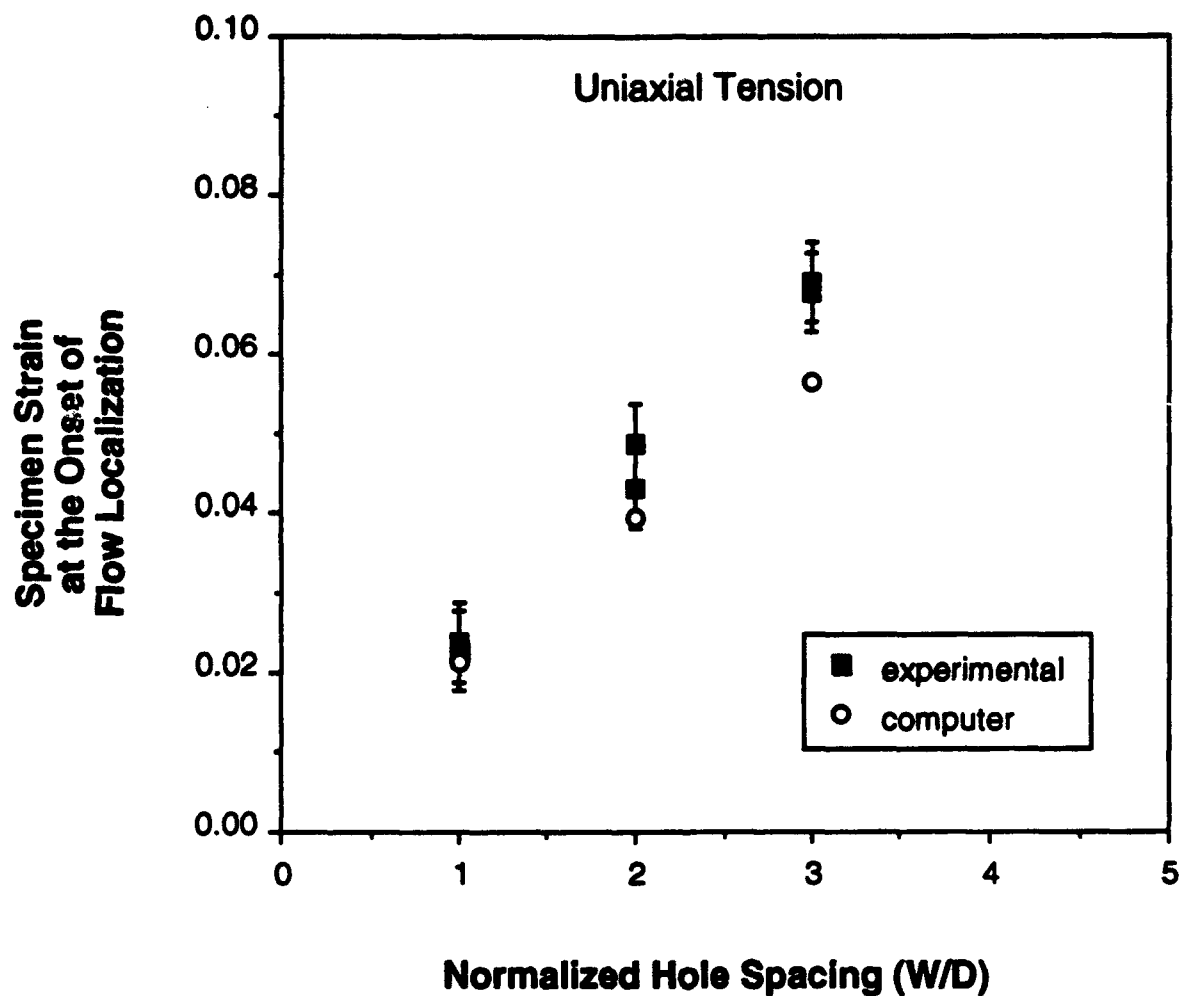


Figure 3: The dependence of the specimen gage-section strain, at the onset of flow localization, on the normalized spacing between a pair of holes. Specimens were deformed in uniaxial tension. The strain-hardening exponent is 0.20. The interhole hole ligament width, W , is normalized by the hole diameter, D .

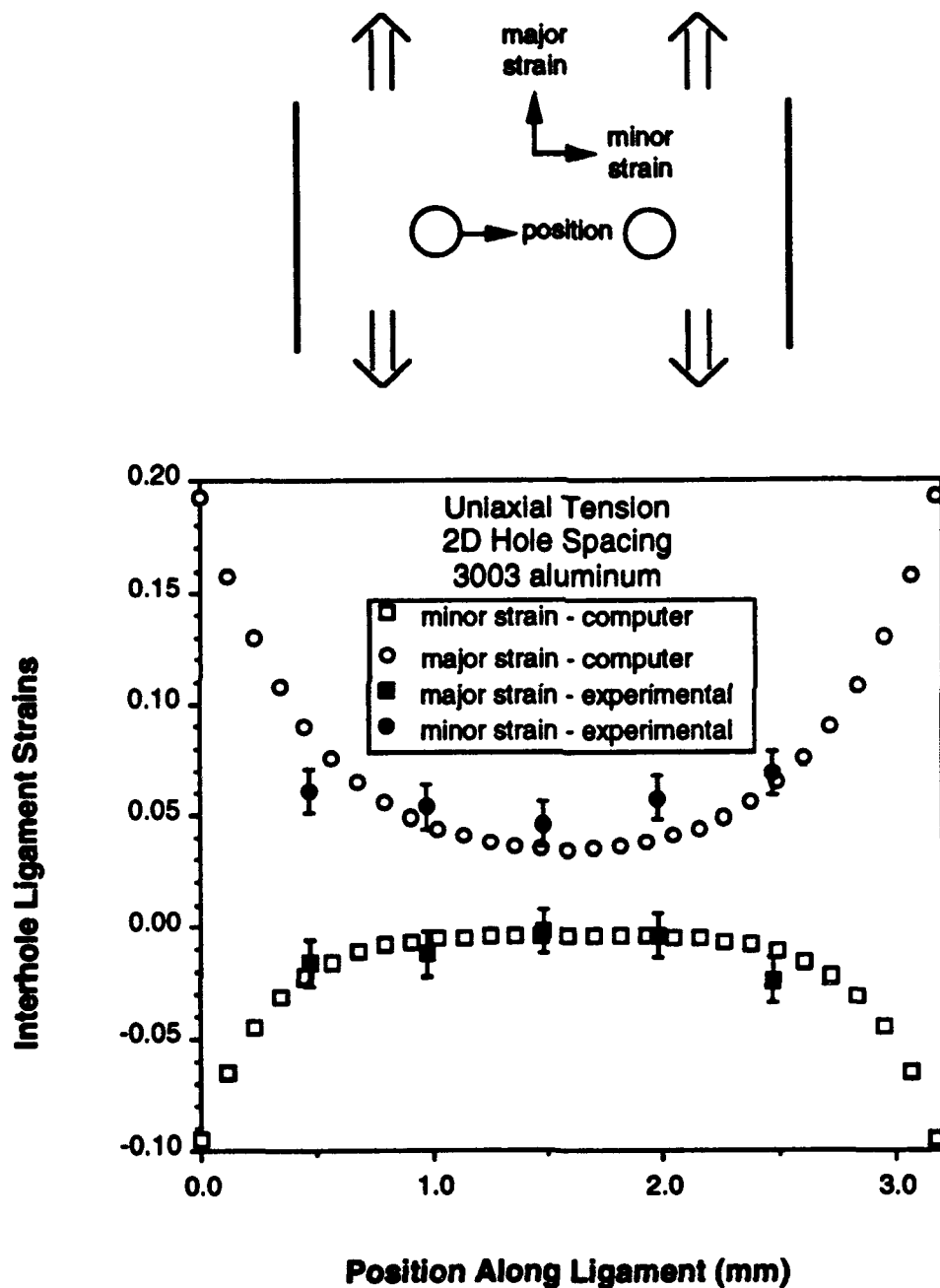


Figure 4: The spatial dependence of the local major and minor strains within the ligament between a pair of holes originally spaced 2 hole diameters apart. The specimen is tested in uniaxial tension.

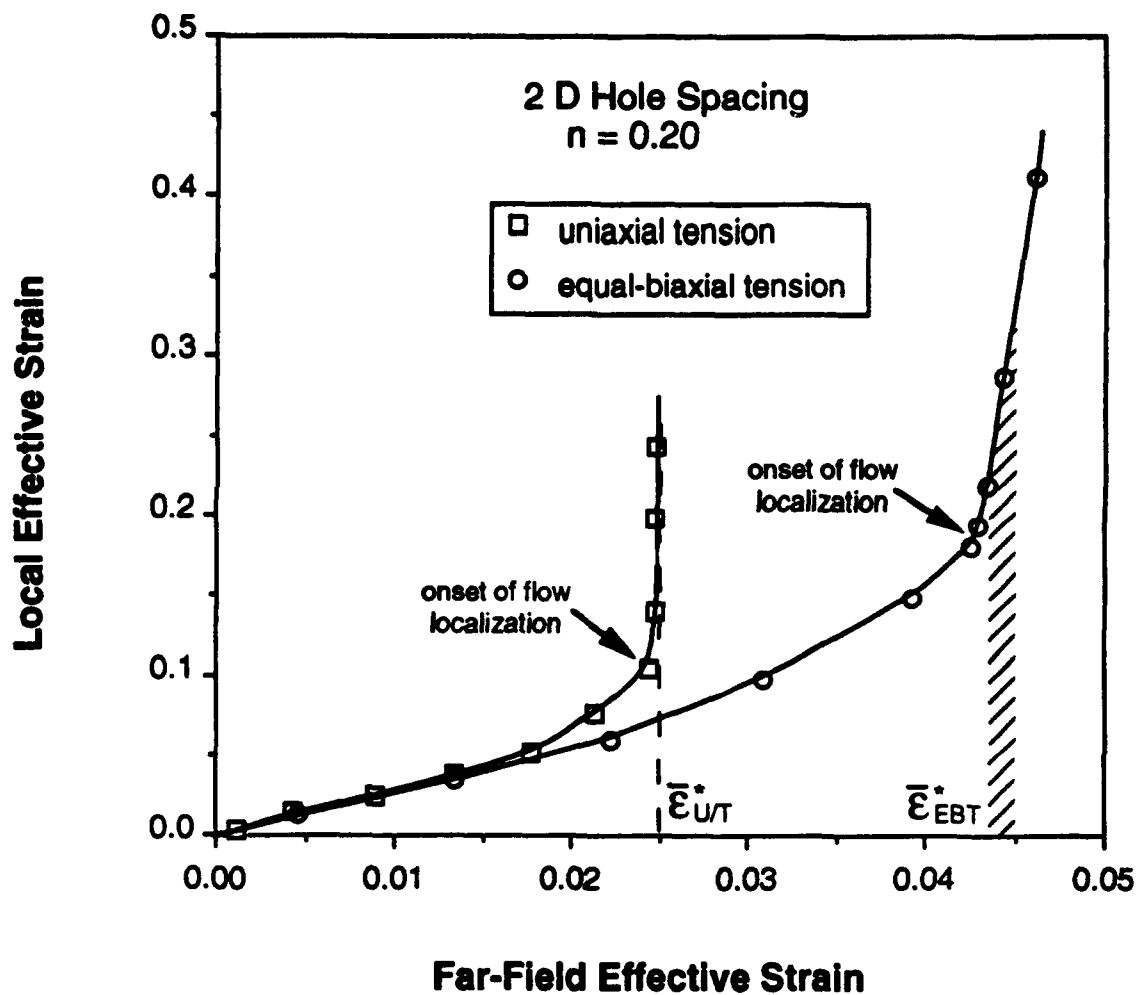


Figure 5: Computational predictions of the evolution of "local" effective strains within an element centrally located between a pair of holes as a function of the imposed far-field effective strain.

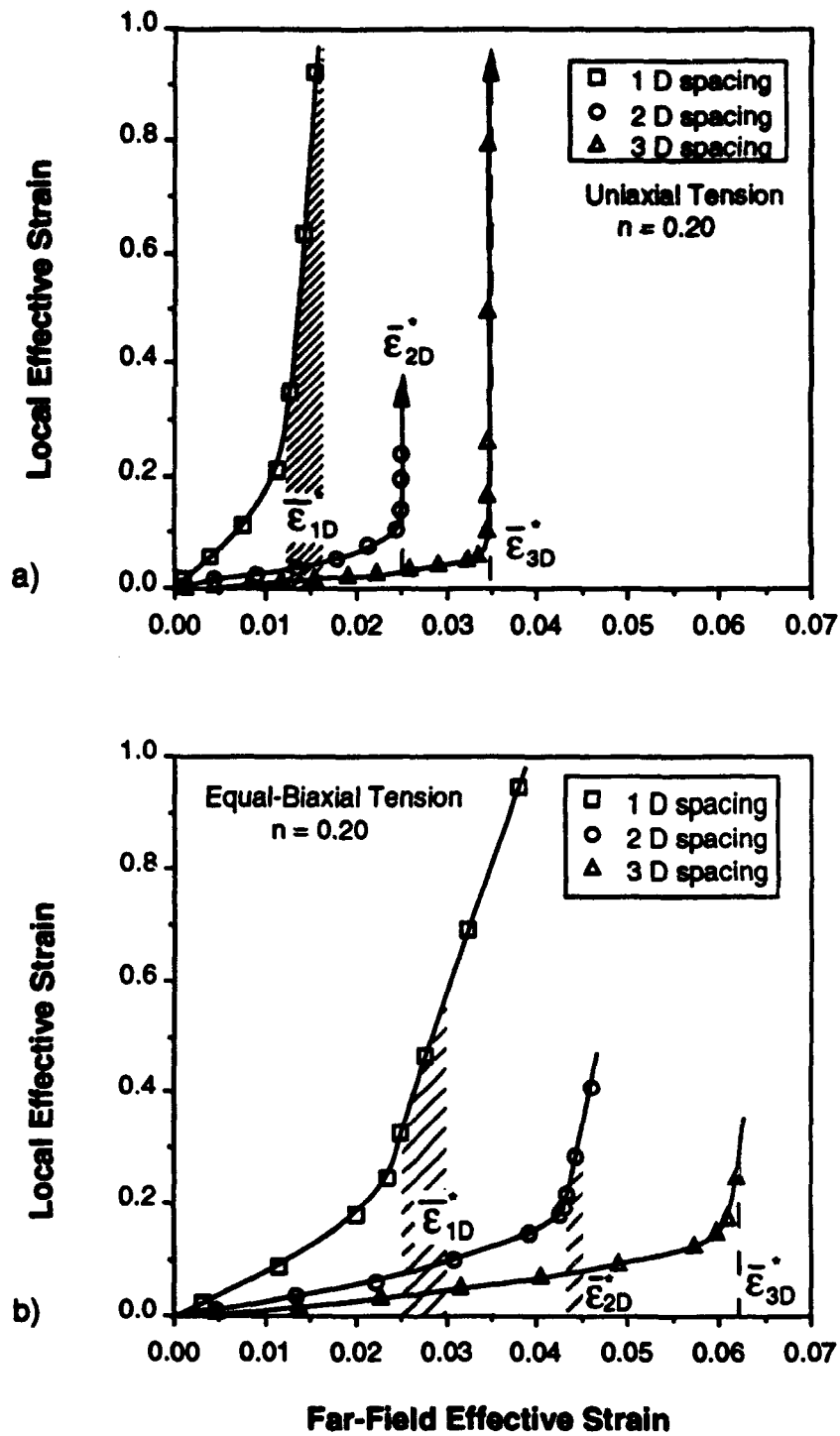


Figure 6: Computational predictions of "local" effective strains within an element centrally located between a pair of holes as a function of the far-field effective strains. The data indicate the influence of hole spacing and contrast the response in uniaxial and equal-biaxial tension.

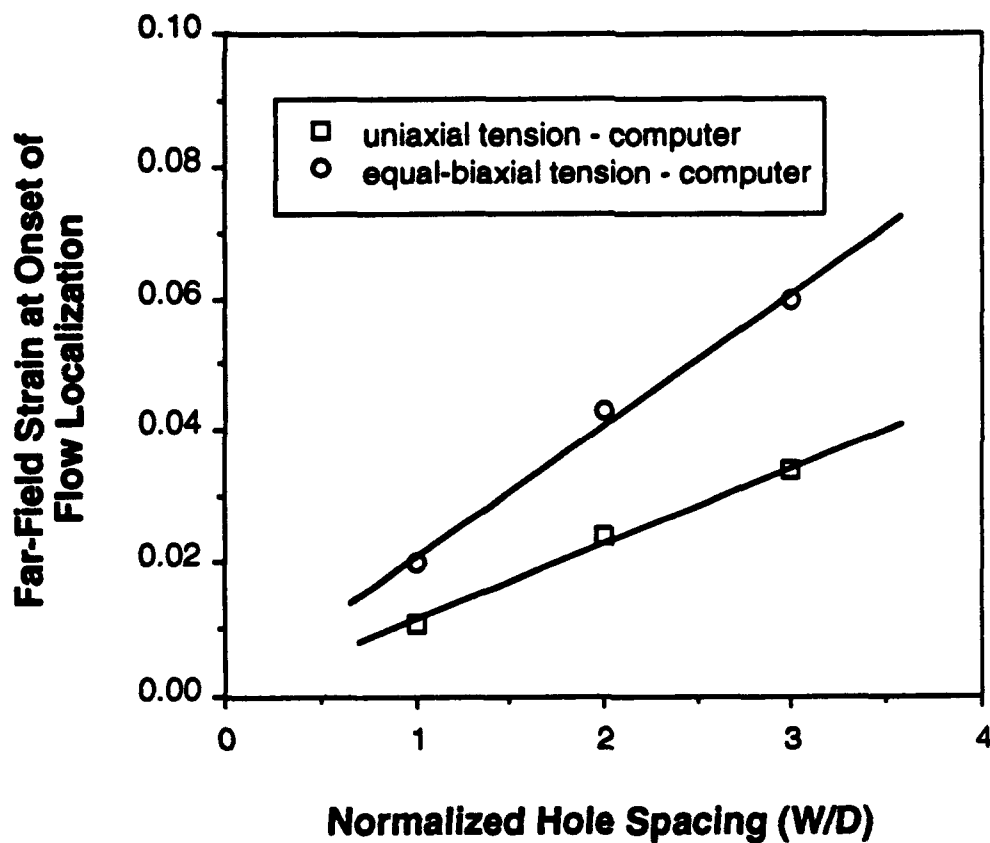


Figure 7: The influence of interhole spacing on the far-field effective strain at the onset of flow localization between a pair of holes. Computational predictions compare responses in equal biaxial tension to those in uniaxial tension for a material with $n=0.20$.

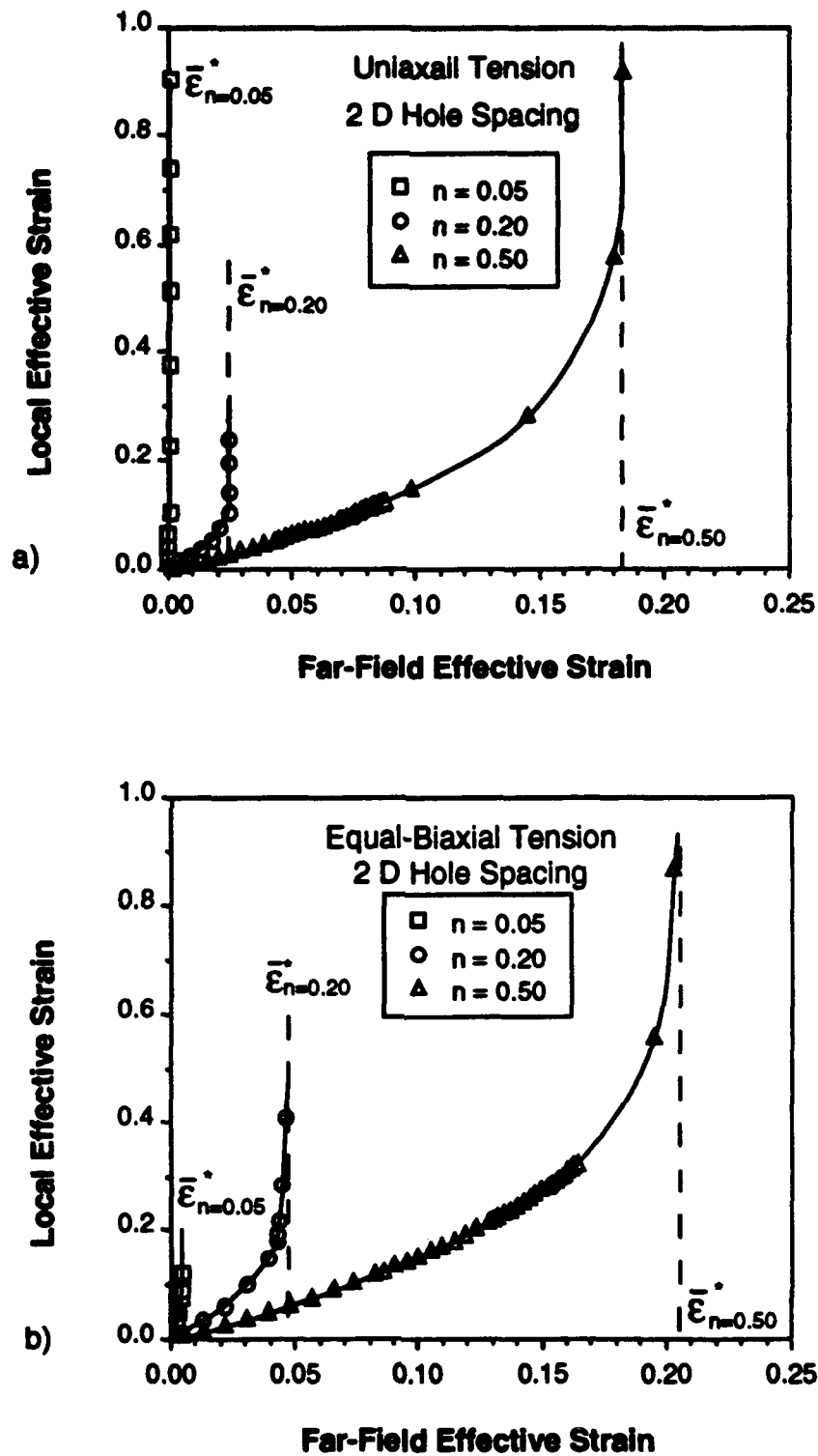


Figure 8: The influence of strain-hardening exponent, n , on strain localization in an element centrally located within the ligament between a pair of holes in a specimen deformed in a) uniaxial and b) equal-biaxial tension.

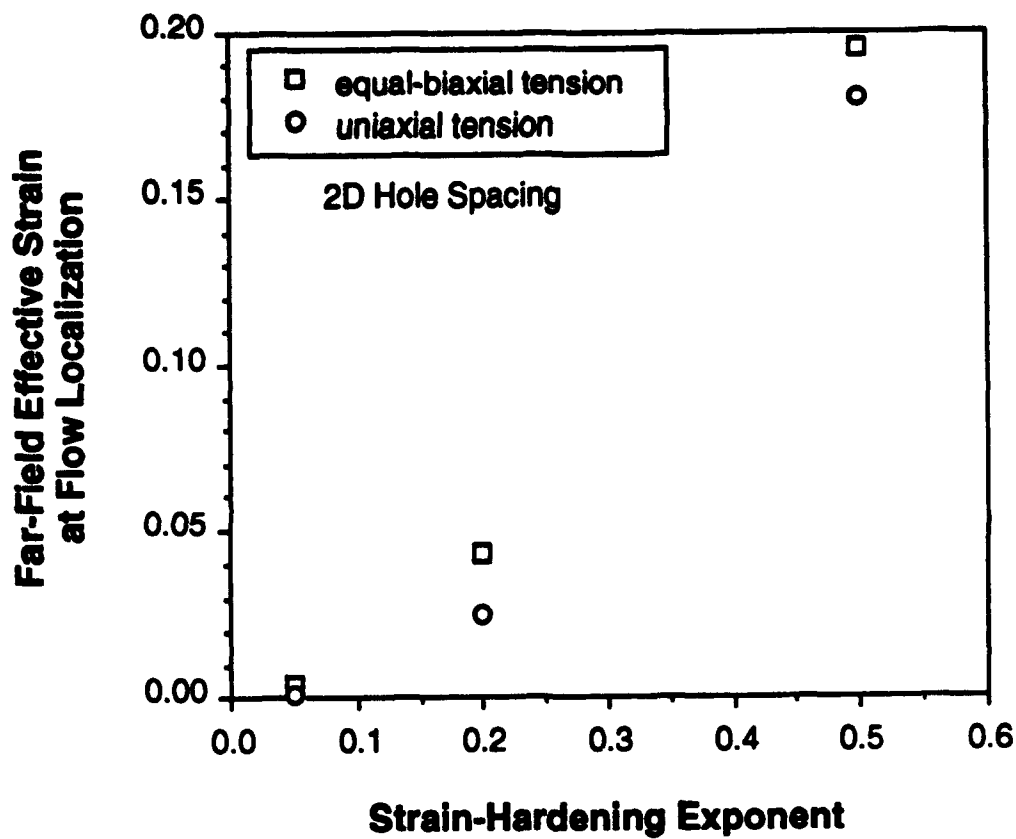


Figure 9: The dependence of the far-field effective strain at the onset of flow localization on strain-hardening exponent for uniaxial and equal-biaxial tension. Data are computed for localization at an element located at the center of the interhole ligament.

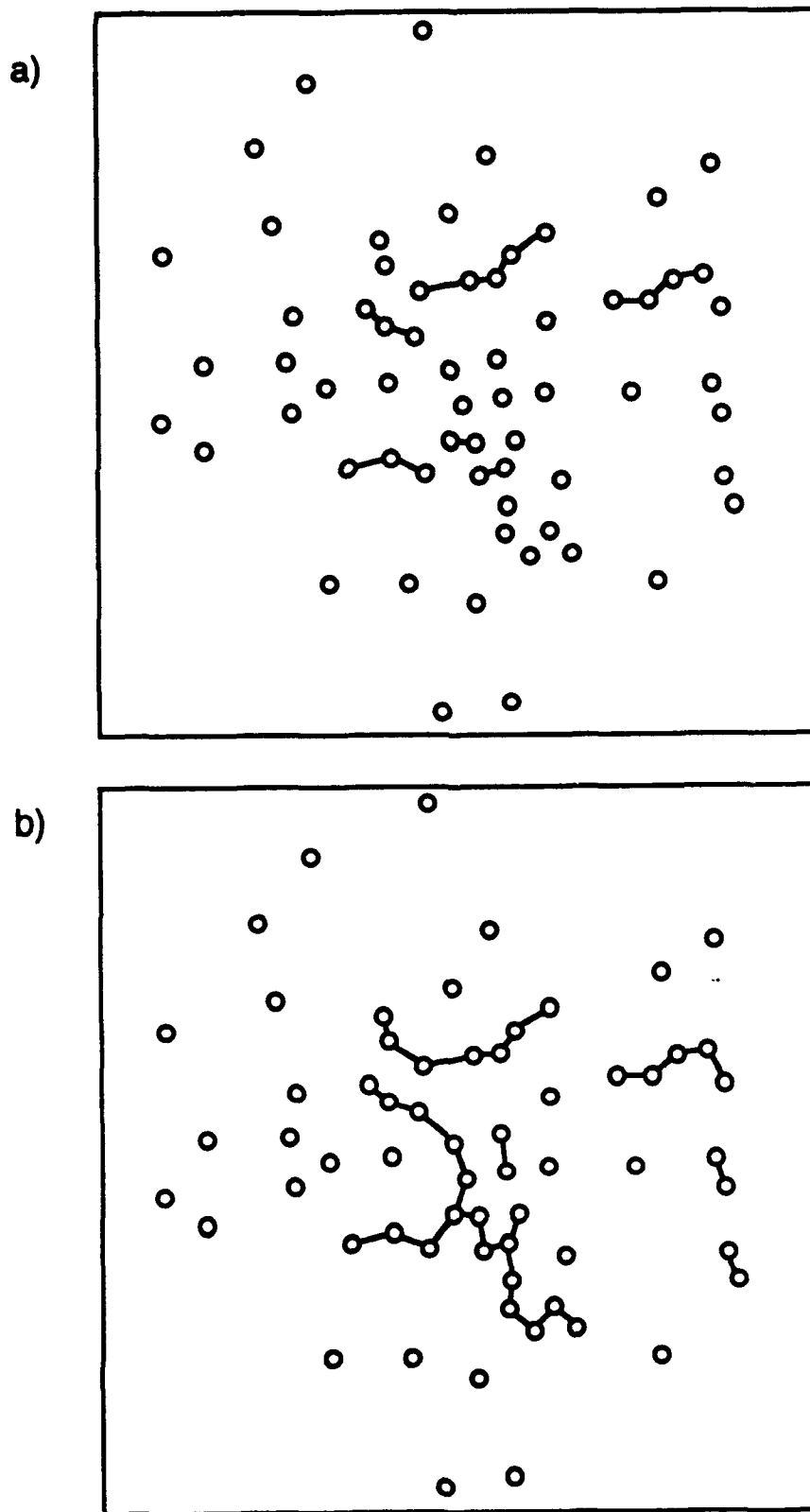


Figure 10: The flow localization paths developed in specimens with a minimum allowable hole spacing of one hole diameter and tested in either a) uniaxial tension or b) equal-biaxial tension. The tensile axis is vertical for the uniaxial case.

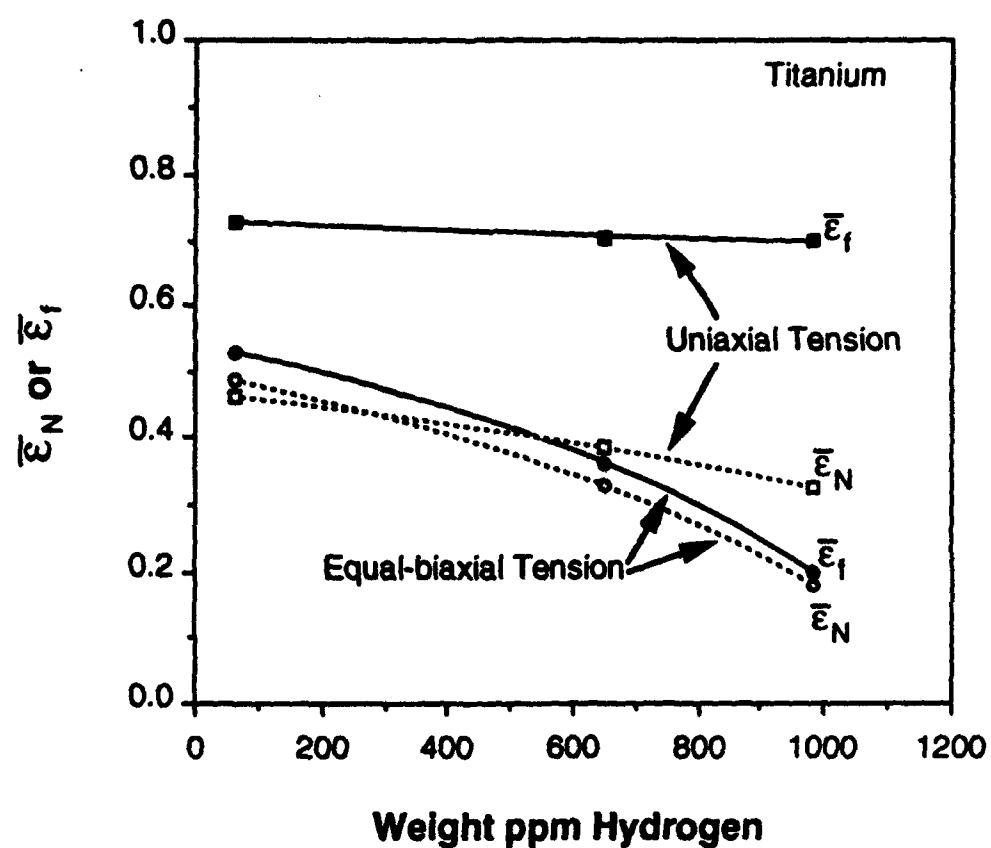


Figure 11. The influence of hydrogen content on the effective strain at either void nucleation, $\bar{\epsilon}_N$, or specimen fracture, $\bar{\epsilon}_f$, of titanium deformed in either uniaxial tension (transverse to the rolling direction) or equal-biaxial tension. After ref. 17.

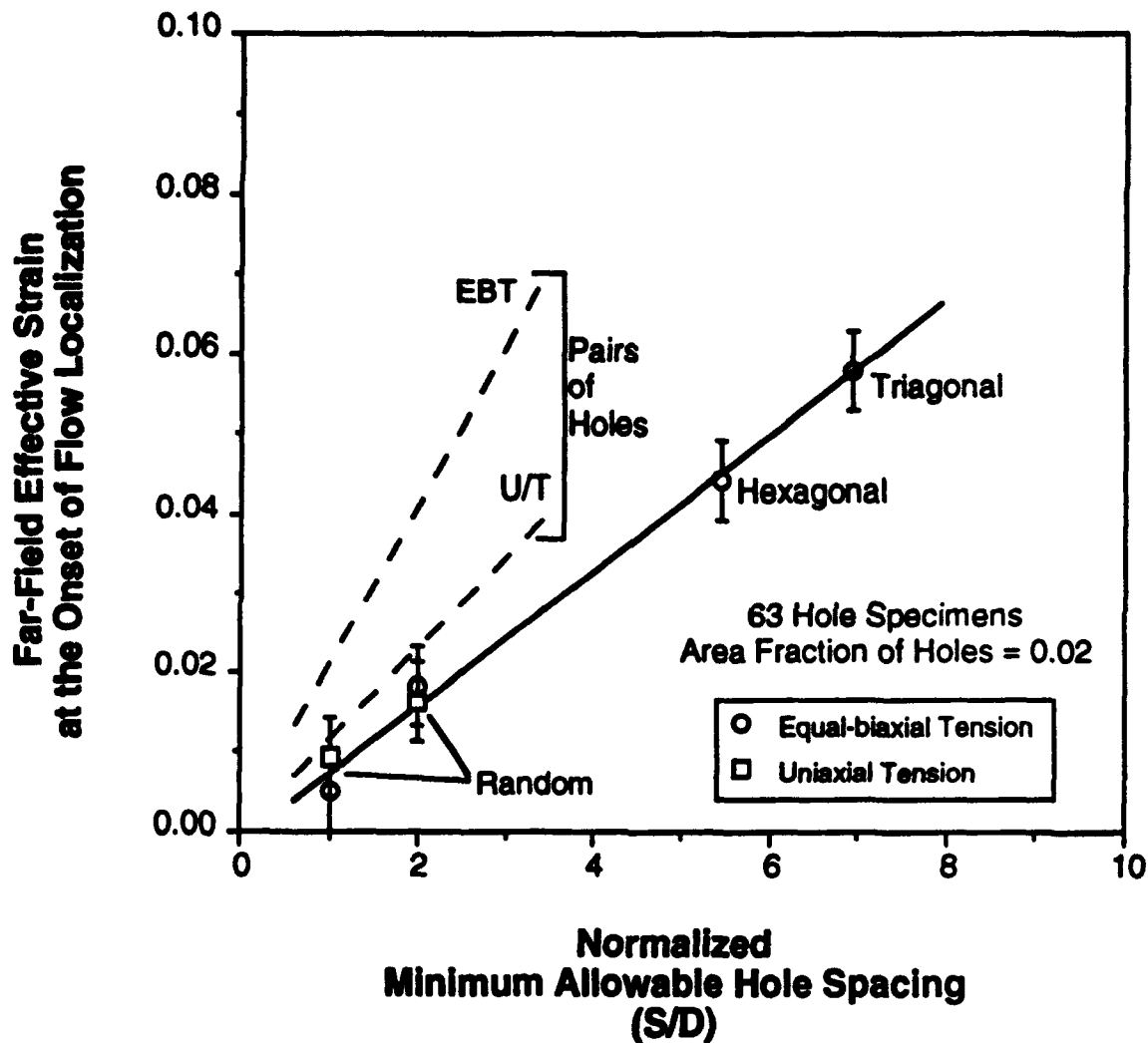


Figure 12

The effect of minimum interhole spacing, S , normalized by hole diameter, D , on the far-field effective strain at the onset of flow localization between holes. The hexagonal and trigonal arrays are regular arrays. Decreasing S/D acts to increase hole clustering. EBT denotes equal-biaxial tension, and U/T denote uniaxial tension.